Climatic Change (2021) 164:57
https://doi.org/10.1007/s10584-021-03028-w

Surface air pressure–based reconstruction of tropical cyclones affecting Hong Kong since the late nineteenth century

Yingxian Zhang[1] · Yuyu Ren[1] · Guoyu Ren[1,2] · Yongqiang Zhang[1]

Received: 6 August 2020 / Accepted: 4 February 2021/Published online: 25 February 2021

Abstract
By using instrumental surface air pressure (SAP) records for 1885–2017 at Hong Kong (HK) station, SAP data for 1951–2016 at 66 stations over mainland China and modern tropical cyclones (TCs) of 1951–2017 derived from the Best Tracks (BT) dataset over Northwest Pacific, an objective identification method (OIM) for TCs is developed. Taking HK station as an example, the general distance of detectable landing TCs and the SAP thresholds are determined by utilizing the correlation between the SAP metrics at HK station and those at each landing site for all 392 real modern TC processes during the period of 1951–2016. Then, a long series of TCs affecting HK station for 1885–2017 is reconstructed by applying the thresholds of daily mean SAP and 24-h SAP difference to observed SAP data during the whole stage. The misjudgment of this OIM is about 10%, and it provides a homogeneous series of TCs affecting HK area during 1885–2017. The reconstructed annual TC series shows a visible decreasing trend from 1885 to 2017, with a more obvious reduction occurring after the early 1960s. Specifically, the 10 years of 1994–2003 had the smallest number of TCs. This SAP-based method developed in this study is potentially applicable for other areas.

Keywords Reconstructed tropical cyclones · Instrumental records · Surface air pressure · Distance of detectable tropical cyclones · Climate variation · East Asia

This article is part of the topical collection on "Historical and recent change in extreme climate over East Asia," edited by Guoyu Ren, Danny Harvey, Johnny Chan, Hisayuki Kubota, Zhongshi Zhang, and Jinbao Li.

✉ Guoyu Ren
guoyoo@cma.gov.cn

1 Laboratory for Climate Studies, National Climate Center, China Meteorological Administration, Beijing 100081, People's Republic of China

2 Department of Atmospheric Science, School of Environmental Studies, China University of Geosciences, Wuhan 430074, People's Republic of China

1 Introduction

As an important part of the global climatic system and one of the main weather and climate extreme events, tropical cyclones (hereafter referred to as TCs) or typhoons can cause severe disasters in tropical and mid-latitude coastal regions, in particular in Western Pacific costal zones. The study on the evolution of TCs is not only of great academic significance in understanding the mechanism of global climate change but also of great practical significance in adapting to climate change and variability and in dealing with natural disasters effectively. It is thus very important to obtain the accurate information of TCs, including the long and homogeneous series of TCs in East Asian coastal regions.

Prior to 1970, however, the typhoon information is considered to be poorer because of the lack of satellite coverage (Liu and Chan 2008). This leads to strong discrepancies in TC statistics and changing trend estimates derived from different observational and reconstructed datasets, including those based on the "Best Track" datasets (hereafter referred to as BT) (Barcikowska et al. 2017). Before the mid-nineteenth century, TCs can only be reconstructed by using other records (non-climatic records or proxy data), such as historical documents (Chan and Shi 2000; Liu et al. 2001; Fogarty et al. 2006; Grossman and Zaiki 2009; Zhang et al. 2012; Pan et al. 2012; Kobayashi and Pan 2014), and marine-derived flood deposits (Ladlow et al. 2019), due to the lack of modern instrumental observations.

As far as China is concerned, the earliest TC records can be traced back to Northern Song Dynasty (AD 960–1126), and most of these records derived from local administrative authorities and gazettes (Louie and Liu 2003; Liu et al. 2001). However, TC counts were likely underestimated prior to 1600 and that storms much weaker than TC intensity may not have been recorded (Fogarty et al. 2006). On the other hand, TC counts in the early stage were less reliable than that in the later period because of societal development and the state of the science (Fogarty et al. 2006). From the late nineteenth century to the mid-twentieth century, TC information usually derived from synoptic charts and early limited instrumental records (e.g., Gao and Zeng 1957; Chin 1972). Nevertheless, TC information coming from different data sources in this period might be inconsistent. Hung (2013) constructed a 300-year series of TCs affecting Taiwan by merging TC records derived from different sources, but the Central Weather Bureau data applied include fewer typhoons during the period 1897–1948, which would probably be due to the lack of modern observation means at that time.

Accordingly, the understanding of long-term variations of TCs as well as the corresponding influence and mechanism is still restricted. Therefore, it is necessary to develop an objective method to identify typhoon processes during the long pre-1950s period by using high-quality observation data and unified identification standard. At present, a certain amount of instrumental records from the late nineteenth century to the early 1950s is being rescued, such as surface air pressure (SAP). This makes it possible to develop such an objective identification technique of TCs.

In view of the above, an objective identification method (OIM) of TCs based on instrumental SAP records was established in this study. This method was then applied to the objective recognition of TCs affecting Hong Kong (HK), as well as the establishment of a long series of annual TC numbers. Taking HK as an example is due to the availability of high-quality and long-term SAP data at present. In Section 2, the dataset and methods utilized are briefly introduced; Section 3 presents the SAP thresholds for the occurrence of CTs affecting HK station and the long-term series of annual TC numbers reconstructed by applying the OIM developed in this study. Discussion and conclusions are provided in Sections 4 and 5.

2 Data and method

2.1 Data

The observed 6-hourly (6-h) local SAP records at 00:00, 06:00, 12:00, and 18:00 UTC from 1885 to 2017 in HK, derived from the International Surface Pressure Databank (ISPD) (version 4, https://reanalyses.org/observations/international-surface-pressure-databank) and the Integrated Surface Database (ISD) (https://www.ncei.noaa.gov/data/global-hourly), were used to identify TCs that have impacts on HK since the late nineteenth century. Meanwhile, the observed 6-h local SAP and daily mean local SAP (the average value at 00:00, 06:00, 12:00, and 18:00 UCT), derived from version 3.0 (V3.0) of the basic meteorology historical dataset of a dense national observational network from 1951 to 2016 over mainland China released by the National Meteorological Information Center (NMIC) of the China Meteorological Administration (CMA) (Ren et al. 2012), were also used in this study. In addition, the BT of TCs over Northwest Pacific from 1951 to 2017 (Ying et al. 2014) released by Shanghai Typhoon Institute (STI) of CMA (http://tcdata.typhoon.org.cn) was used to determine the SAP thresholds of target stations affected by TCs. The landfall information of TCs, including the first landfall site and date, was derived from Meteorological Disaster Risk Management System (MDRMS) developed by National Climate Center, CMA. MDRMS collected the detailed summaries of TCs in Northwest Pacific during the period of 1949–2016. According to the BT dataset and the landing information of TCs, a total of 392 landing TCs from 1951 to 2016 and 67 landing sites (including HK) over mainland China (Fig. 1) were extracted. Then, SAP records (including 6-h and daily mean values) during the 9-day landing period (from 4 days before to 4 days after TC landing) at 67 landing sites for each landing TC were extracted. These SAP series will be used to determine the general distance within which TCs could be detected by using local SAP records as well as the corresponding thresholds at HK station.

2.2 Method

In view of inconsistent variables at HK station (Table 1), an empirical formula was utilized to adjust all the local SAP data during the period of 1885–1939 to the local sea level pressure (SLP). The static equation presents the variation of air pressure with altitude (Zhu et al. 2000)

$$0 = -\frac{1}{\rho}\frac{\partial p}{\partial z} - g \qquad (1)$$

where p, z, ρ, and g are the air pressure, the altitude, the density of air, and the gravitational acceleration, respectively. In this study, we set $\rho = 1.29$ kg/m^3 and $g = 9.81$ m/s^2. Further, Eq. (1) can be transformed to

$$p_2 - p_1 = -\rho g(z_2 - z_1) \qquad (2)$$

$$p_2 - p_1 = -12.7(z_2 - z_1) \qquad (3)$$

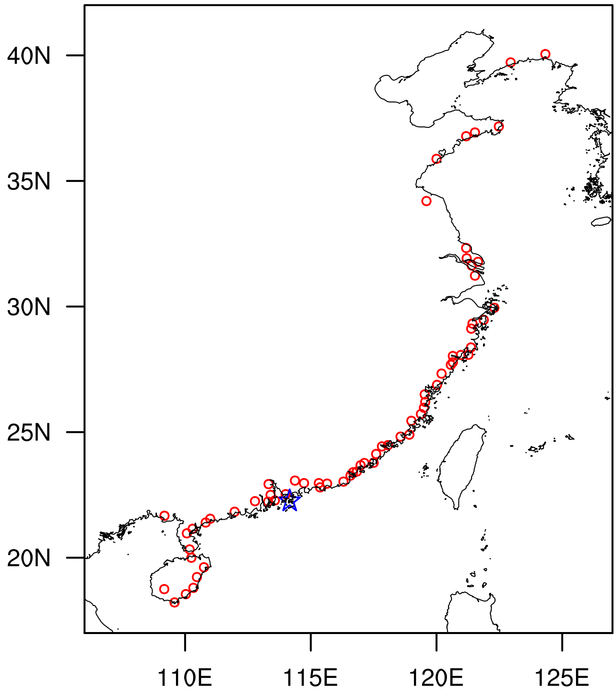

Fig. 1 Sixty-seven landing sites of TCs (red circles) over mainland China during 1951–2016 (the blue star is HK station)

where z_1 and z_2 are the altitude of levels 1 and 2; p_1 and p_2 are air pressure on levels 1 and 2. Equation (3) indicates that the air pressure drops by 12.7 Pa or 0.127 hPa every 1 m of height rise. Finally, the adjustment equation can be transformed to

$$P_{adj} = P_{obs} + H_{obs} \times 0.127 \tag{4}$$

where P_{adj} and P_{obs} are the adjusted local SLP and the observed local SAP, respectively (in hPa), and H_{obs} is the altitude of the station (in m). Accordingly, a time series of local SLP from 1885 to 2017 at HK station was generated. The homogeneity of the daily SLP series at HK station from 1885 to 2017 (Fig. 2) was tested by RHtests software (Wang et al. 2010), and no inhomogeneous points were found.

The flow chart of the TC reconstruction method developed in this study is displayed in Fig. 3. We firstly calculated the SAP thresholds at HK station when one landing TC nearby has potential impacts on it or the TC can be detected, according to the information in 392 modern landing TCs, the observed SAP variations at HK station, and the landing sites. Then, the SAP thresholds determined were applied to the long series of SAP records during 1885–2017 at HK

Table 1 The information of HK stations

Station name	Latitude (° N)	Longitude (° E)	Altitude (m)	Period (year.month)	Variable	Source
Hong Kong (HK)	22.3	114.17	62.0	1885.1–1939.12	Local SAP	ISPD
	22.3	114.17	62.0	1947.1–2009.12	Local SLP	
Sha Tin (ST)	22.4	114.2	8.0	2010.1–2017.12	Local SLP	ISD

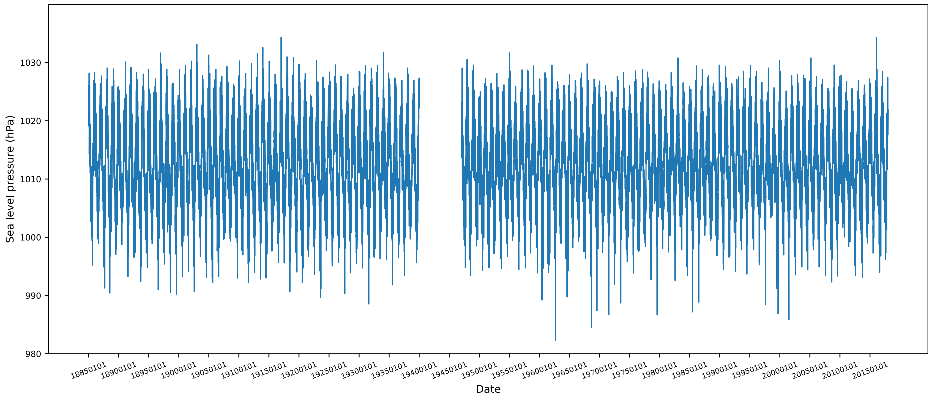

Fig. 2 The time series of daily SLP at HK station from 1885 to 2017 (the records from 1940 to 1946 are missing)

station. Finally, the TCs having impacts on HK station during the long-term period of 1885–2017 were reconstructed.

The concept of correlation decay distance (hereafter referred to as CDD), also called correlation length scale or decorrelation length (Hofstra et al. 2008), was utilized to judge the distance of detectable landing TCs by using SAP records and to determine the SAP thresholds at the target station in this study. For the target station, the landing TCs within CDD were supposed to have impacts on the observational site in terms of SAP, and vice versa. The CDD is usually defined as the distance where the correlation of SAP series between target station and all other stations decays below one specific value (Briffa and Jones 1993; Jones et al. 1997; Hofstra et al. 2008; Zhang et al. 2017a).

Firstly, the Pearson correlation coefficients of SAP series at the target station and each other station were determined. Then, the coefficients were sorted by spherical-geometry distance (Willmott et al. 1985) to the target station and one appropriate function was fitted by the least squares method to the cloud of points. Finally, the CDD was set to the distance where the

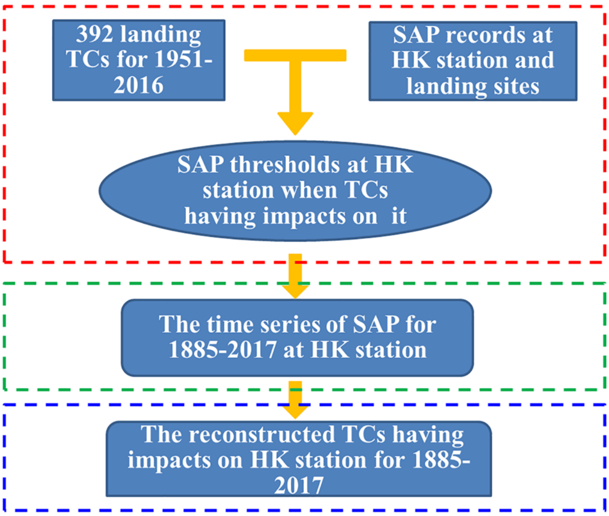

Fig. 3 The flow chart of TC reconstruction affecting HK station

correlation is approximately equal to the 0.05 significance level for the correlations with large samples.

3 Results

3.1 CDD of TCs

As described in Section 2.2, the key to the TC reconstruction is how to select the appropriate SAP metric for determining the corresponding threshold. We found that the absolute value of 6-h local SAP difference (i.e., the absolute value of SAP difference between the current time and 6 h ago) at the landing site on the day of landfall was much greater than that on the other days (Fig. 4). The absolute value of 6-h SAP difference apparently rose when TCs approached the landing sites, and the maximum value can reach more than 50 hPa in extremity on the landing day. After landing, the absolute value of 6-h SAP difference at the landing sites gradually dropped. Theoretically, there is a high correlation between the variation of the absolute value of 6-h SAP difference at the landing site and that at the station nearby, and vice versa. In other words, the closer the distance between the landing site and target station, the higher the correlation of the absolute value of 6-h SAP difference between them. Besides, the correlation coefficient also depends on the strength of TC and the direction of TC movement.

Take HK station as the target station. The ΔSLP (i.e., the absolute value of SLP difference between the current time and 6 h ago) series at HK station during the 9-day landing period (from 4 days before to 4 days after TC landing) for each landfall TC was generated. Following this, the ΔSAP series during the landfall period at the landing site for each landfall TC was also be generated. Then, the Pearson correlation between ΔSLP series at HK station and ΔSAP series at landing site during the landfall period for each landing TC was calculated. The

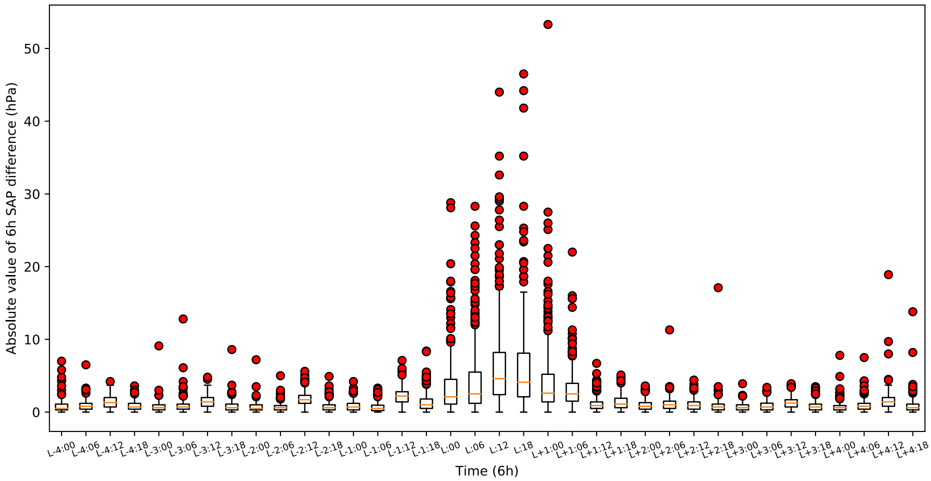

Fig. 4 The variation boxplot of the absolute value of 6-h SAP difference at landing sites during the 9-day TC landing period (from 4 days before to 4 days after TC landing) for 392 TC landfalls. Boxes indicate the interquartile model spread (25th and 75th quantiles) with the orange horizontal line indicating the median, the whiskers showing the extreme range, and red dot indicating the outlier

exponential, logarithmic, and linear functions were fitted by least squares to the cloud of correction points, and the exponential function was eventually chosen due to the highest goodness of fit (Table 2)

$$r = e^{-px} \tag{5}$$

where x is the distance between the target station and the landing site, r is the correction of ΔSAP series between them, and p is the fitting coefficient. The CDD therefore corresponds to the distance where r is equal to the 0.05 significance level ($r = 0.329$ for $N = 36$). For HK station, the CDD is 362 km (Fig. 5), which means that TCs within this distance could have significant impacts on HK in terms of the variation of ΔSAP.

3.2 SLP thresholds

For HK station, the daily mean SLP and the absolute value of 24-h SLP difference were chosen as the key metrics, and their appropriate thresholds for TCs that have impacts on HK were determined. Daily mean SLP is the average value of SLP at 00:00, 06:00, 12:00, and 18:00 UTC, and the absolute value of 24-h SLP difference was the absolute value of SLP difference between the current day and the previous day. The minimum value of daily mean SLP and the maximum value of the absolute values of 24-h SLP difference at HK station during the 3-day landing period (from 1 day before to 1 day after TC landing) of each landing TC are plotted against the distance from the landing sites in Fig. 6. The cloud points were fitted by two fitting functions (exponential and logarithmic functions) according to the least squares method, and the goodness of fit is calculated (Table 3). We found that the exponential function had a higher R^2 value than the logarithmic function did (Table 3), so the exponential function was eventually chosen for fitting (see blue curves in Fig. 6). Accordingly, the exponential functions of CDD were considered to be the thresholds of the corresponding SAP metrics (i.e., the corresponding function value to the intersection of the blue curve and the black dashed line in Fig. 6). Following the above steps, the thresholds of daily mean SLP and the absolute value of 24-h SLP difference at HK station were determined, i.e., 1004.2 hPa and 3.4 hPa, respectively (Fig. 6).

3.3 TC identification

Following Section 3.2, the thresholds for two metrics at HK station were determined. Daily mean SLP and 24-h SLP difference at HK station during 1885–2017 were used to identify the historical TCs that have impacts on it. We defined that if the mean SLP on one certain day is below 1004.2 hPa while the 24-h SLP difference on that day or 1 day before is below −3.4 hPa at HK station, HK station on that day is supposed to be affected by a TC. In addition, when the mean SLP on one certain day is below 1004.2 hPa, however, the 24-h SLP difference on that

Table 2 The corresponding goodness of fitting functions (R^2) for the correlation points in Fig. 5

Fitting function	Goodness of fit (R^2)
Exponential $y = e^{-px}$	0.61
Logarithmic $y = a\ln x + b$	0.55
Linear $y = ax + b$	0.36

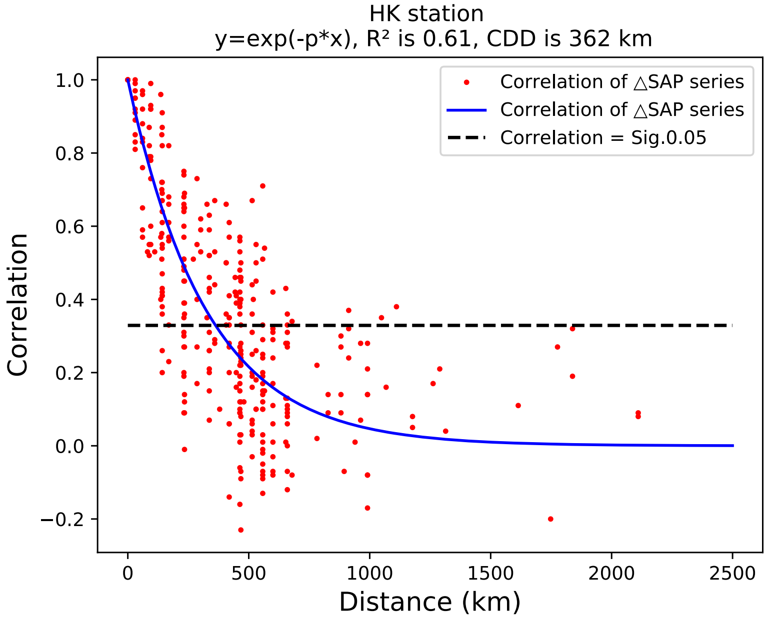

Fig. 5 CDD (km) at HK station using the series of the absolute value of 6-h SAP difference during the 9-day landing period

day or the previous day is negative but higher than −3.4 hPa; a TC is also supposed to affect HK if the 24-h SLP difference on 1 day after or 2 days after is larger than 3.4 hPa. According to the abovementioned procedure, it is possible to determine whether HK station on one certain day had been affected by a TC. When HK on successive days or 1-day interval are determined to be affected by possible TCs, one TC is identified; otherwise, the new TC is identified.

During the period of 1954–2017, a total of 266 TCs that have impacts on HK station was identified by using the SLP thresholds determined in Section 3.2. In order to examine the effectiveness of this identification method, a check was conducted by comparing with the BT

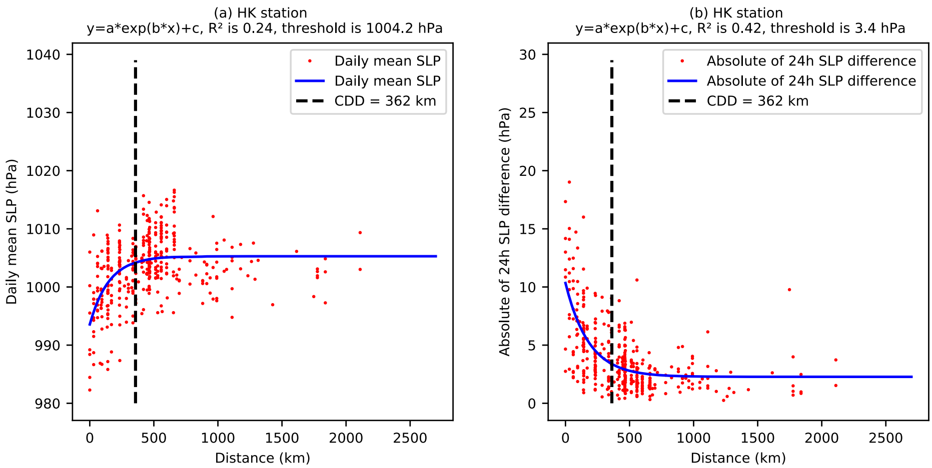

Fig. 6 The **a** daily mean SLP and **b** the absolute value of 24-h SLP difference thresholds at HK station

Table 3 The corresponding goodness of fitting functions (R^2) for the SLP metrics in Fig. 6

Fitting function	Daily mean SLP	Absolute of 24-h SLP difference
Exponential $y=ae^{bx}+c$	0.24	0.42
Logarithmic $y=a\ln bx+c$	0.15	0.37

over mainland China from 1954 to 2017. Upon verification, 241 of the identified 266 TCs really existed; however, 25 objectively identified TCs by using the SLP thresholds did not exist in reality. That is to say, the misjudgment rate of this TC identification method is about 10%. The false identifications may be related to the influence of mesoscale to small-scale weather systems, such as vortex, low-pressure trough, and so on, approaching HK station. Meanwhile, a few of real TCs were not detected by this method. Compared with the TCs in BT crossing within the CDD (i.e., 362 km) of HK, about 30% of the TCs stronger than severe tropical storm were not objectively identified. This is because the SLP records at HK station did not reach the defined thresholds, though these TCs have once entered the range. That is to say, these TCs did not have a significant influence on SLP change of HK. Some of these TCs did not land in China, some landed far away from HK station, and some weakened significantly as they approached the continent. It seems that the stronger TCs or the TCs passing closer to HK are more likely to affect the SAP change in HK.

Compared with the annual 6.1 TCs during 1961–2010 documented by Hong Kong Observatory (HKO) (https://www.hko.gov.hk/en/education/tropical-cyclone/classification-naming-characteristics/00161-typhoon-56-average-number-of-tropical-cyclones.html), our result (annual 4.3 TCs in Fig. 7) is 1.8 less. One reason is that the result from HKO includes the TCs crossing within 500 km of HK, but the distance of detectable TCs for HK is 362 km in this study. Another reason is that the weak TCs, such as tropical pressure, are

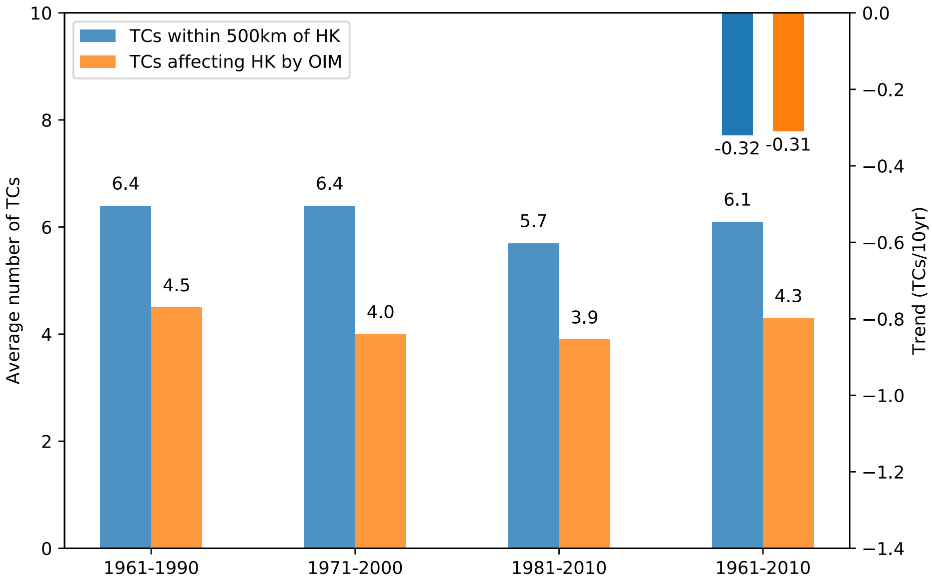

Fig. 7 The average numbers and trends of TCs that have impacts on HK during different periods derived from different sources (orange bars indicate the results derived from OIM of this study, and cyan bars indicate those from HKO)

included in the results of HKO, but some of these TCs cannot be objectively identified by using SLP records of HK due to their weak influence on SLP change at HK station. However, Fig. 7 shows that the 30-year average decreases from the 4.5 for the period of 1961–1990 to 3.9 for 1981–2010. This decadal decline trend is well consistent with the result of HKO. Moreover, the trend of −0.31 TCs per 10 years during 1961–2010 derived from this study is also consistent with that from HKO (−0. 32 TCs per 10 years) (Fig. 7).

3.4 TC series from 1885 to 2017

A long series of annual TCs from 1885 to 2017 was obtained by applying the SLP thresholds to the SLP records during the whole stage (Fig. 8). Unfortunately, the information of TCs from 1940 to 1946 is missing due to the lack of instrumental SAP records at HK station. Figure 8 shows that the number of annual TCs affecting HK decreased since 1885 by a rate of −0.08 TCs/10 years, in spite of the fact that the trend is statistically insignificant. The decreasing trend is also apparent after the early 1960s. The estimate of the trend is supposed to be immune to the missed data of the middle 1940s, because the record-missing period is only 7 years and is located almost in the middle of the whole TC series. The mean of annual TCs from 1885 to 1939 was 4.8, and that from 1953 to 2017 was 4.2. The maximum number of annual TCs having impacts on HK was 10 in 1898 and 1974, and the minimum was 0 in 1886 and 1987. The annual TC series also exhibited obvious inter-annual and inter-decadal variability (Fig. 8). Ten years from 1917 to 1926 registered the most frequent TCs (5.6), and the 10 years from 1994 to 2003 had the smallest number of TCs (3.3) affecting HK. It is also notable that the number of TCs that have impact on HK dramatically decreased after 1993, and the number is higher than the climatological mean of 1885–2017 only in 4 of the 24 years.

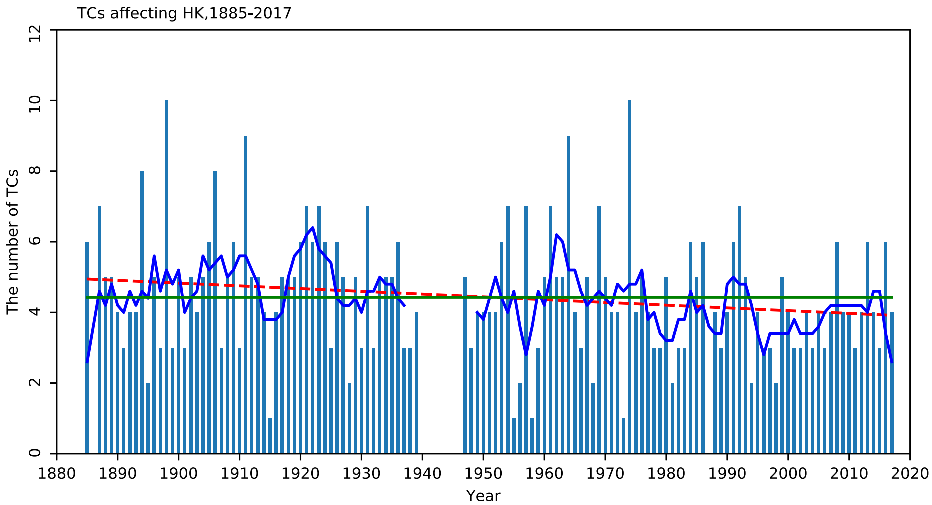

Fig. 8 Annual number (cyan bars) of reconstructed TCs affecting HK station by the OIM in this study for 1885–2017 (SAP records are missing during 1940–1946). Green line, blue curve, and red dashed line depict the climatology, the 5-year running mean, and the liner trend during the corresponding stage, respectively

4 Discussion

The method developed in this work, like any others reported for reconstructing TCs of early time period, has its own shortcomings. Compared to the real TCs over western North Pacific, about 30% of real TCs stronger than severe tropical storm within the CDD (i.e., 362 km) of HK were not objectively identified by this new method. SLP records at HK stations did not reach the defined thresholds though these TCs have once entered into 362 km with HK. That is to say, not all the TCs within the CDD could result in the significant change of SAP at HK station. We have tested the results by changing the thresholds slightly (e.g., changing 1004.2 to 1004.4 hPa; −3.4 to −3.2 hPa). However, doing so did not substantially reduce the number of missed real TCs as well as the rate of misjudgment. Changing the thresholds greatly (e.g., changing 1004.2 to 1006.0 hPa; −3.4 to −2.2 hPa), on the contrary, greatly increased the misjudgment rate or the number of missed real TCs. In addition, we do not particularly know the details of TC landfalls in the 1900s, because of the lack of such information. This leads to an uncertainty about how to adjust the determined thresholds and apply them to the early stage. Most importantly, that different thresholds are applied to different stages might result in the systematic bias between different stages. This kind of bias might confuse the real cause of the long-term variation of TCs. Because of the above reasons, we used the same SAP thresholds during the whole period.

Considering more climate variables, such as wind direction, wind speed, and precipitation, would be helpful to reduce the uncertainty (Kumazawa et al. 2016). However, instrumental wind direction, wind speed, and precipitation data in early years are unavailable for the time being, and we had to use only SAP data to develop the method for reconstructing TCs. Hopefully, the digitized and homogenized data of these records, including the early-year SAP data from other stations, and precipitation and surface wind data for all stations, will be available with the progress of the Atmospheric Circulation Reconstructions over the Earth (ACRE) China, which is focused on rescuing and digitizing sub-daily or daily observational records at stations of China as well as the neighboring countries and regions for the pre-1950 period (Williamson et al. 2018).

The 10% misjudgment rate in present work may have been caused by the mesoscale to small-scale intense convection weather processes. How to eliminate the influence of the mesoscale to small-scale weather systems on the reconstruction also needs to be addressed in the future study. However, this systematic bias of overestimate may not significantly affect the analysis of long-term trend and decadal to multi-decadal variation of the TCs in the area, given the relatively unchanged trend of the local disturbances throughout the 133 years. Of course, the assumption of unchanged local disturbances may not be valid, because some analyses of change of thunderstorms and lightning frequency showed a significantly decreasing trend over the last decades in China including southern part of the country (Zhang et al. 2017b; Xue et al. 2019), implying that the mesoscale to small-scale strong convection activities were becoming weaker with time over southern China coastal areas. If the mesoscale to small-scale intense convection weathers could cause the misjudgment of the reconstructed TCs, the recent decline of thunderstorms and lightning frequency may have been one of the main reasons for the remarkable decrease in the reconstructed TCs in the study area. However, a northward shift of TC occurrences in recent decades was observed and the landfalling TCs in whole China has indeed decreased after 1997 (Fig. 9a), which means that the downward trend of TCs affecting HK is likely real.

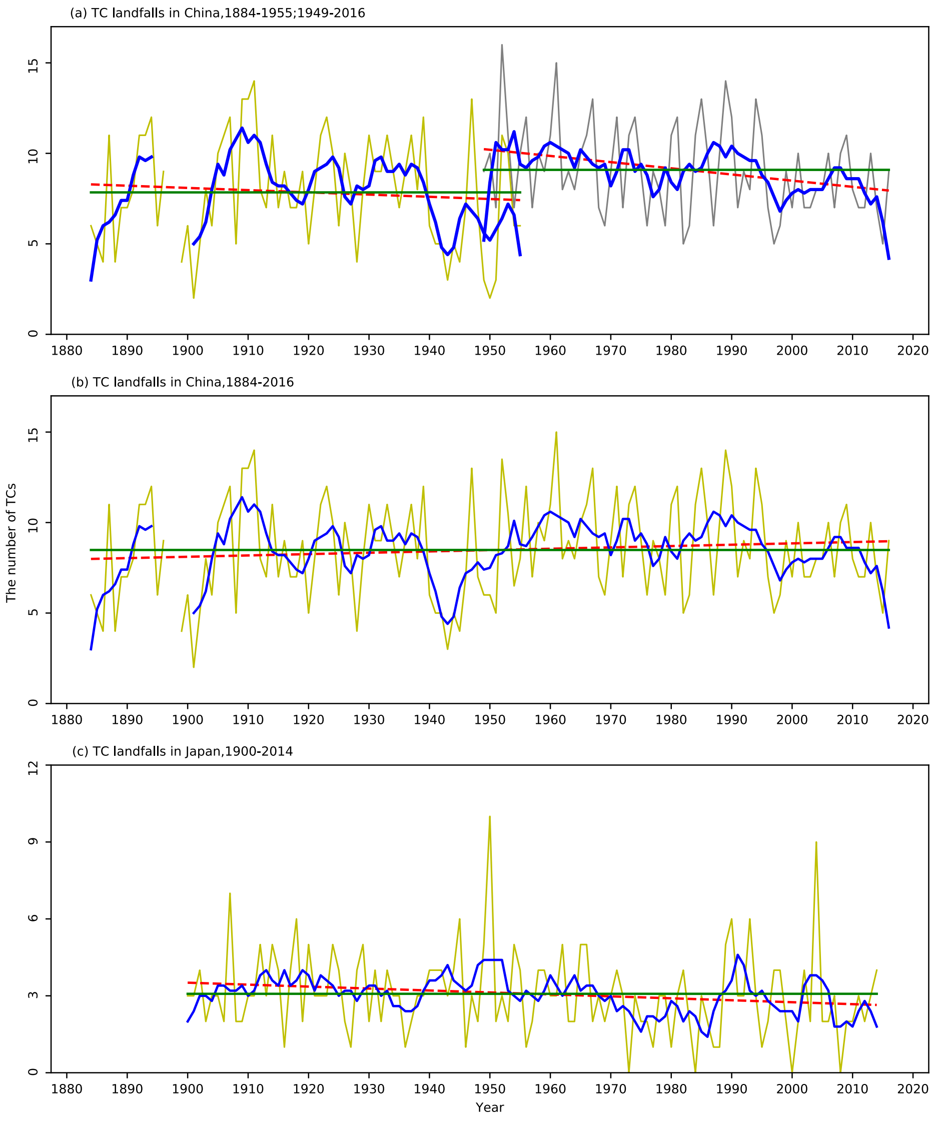

Fig. 9 Sample long TC time series. **a** The annual number of TC landfalls in China for (yellow curve) 1884–1955 (derived from Gao and Zeng 1957) and (gray curve) 1949–2016 (derived from the CMA-BT). **b** The annual number of TC landfalls in China for 1884–2016 by combining the two time series in **a** (yellow curve), and the number of TCs in the overlapping period is the average value from the two sources. **c** The annual number (yellow curve) of TC landfalls in Japan for 1900–2014 (digitalized from Kumazawa et al. 2016). Green line, blue curve, and red dashed line depict the climatology, the 5-year running mean, and the liner trend during the corresponding stage, respectively

Compared to the TC series in Fujian Province as reported in Gao et al. (2007), the reconstructed series of annual TC numbers in this study experienced the similar inter-decadal to multi-decadal variation, e.g., less TCs were detected from the late 1880s to the early 1900s, and more TCs were found from the early 1900s to the early 1930s. It was documented that the number of TCs affecting Fujian Province was less than the climatology during 1932–1955 (Table 4). Hence, according to the low-frequency variation of the reconstructed TC series as well as the variation in TCs affecting Fujian Province, it is likely that the number of annual TCs affecting HK area from 1940 to 1946 was also less than the climatological mean. Gao et al. (2007) showed more TCs during 1956–1971 and less during 1972–2003. However, the number of annual TCs affecting HK fluctuated on multi-decadal scale from the middle 1950s to the early 2000s. This may reflect the discrepancies in the number of TCs affecting different areas of southern China, which may be due to the different landing positions and moving paths of TCs in different periods.

We also made a comparison of our results with those reported by other previous studies for a few areas of East Asian region (Table 5). Figure 9 shows the series of TC landfalls in China derived from Gao and Zeng (1957) during 1884–1955, and from the CMA-BT during 1950–2016 (http://tcdata.typhoon.org.cn) (Ying et al. 2014), as well as the combined series of TC landfalls in China and TC landfalls in Japan (Kumazawa et al. 2016) for the last 100 years plus. For the first half period (1885–1939), annual TC landfalls in China as presented by Gao and Zeng (1957) had an increasing trend by a rate of 0.42 TC per 10 years. However, annual TC numbers affecting HK station by the OIM showed no obvious trend in this period. For the second half period (1949–2016), however, annual TC landfalls in China as given by the CMA-BT exhibited a significantly decreasing trend by a rate of −0.34 TC per 10 years. The TC numbers having influences on HK showed the similar declined trend. Remarkably, the number of annual TC landfalls in China in the overlapping period (1949–1955) derived from the two sources was inconsistent (Fig. 9a), most probably due to different statistic techniques and more information sources in the CMA-BT. This inconsistency undoubtedly could induce the inhomogeneity in the long series of TC landfalls in China. In our opinion, therefore, the increasing trend of 0.07 TC per 10 years simply by combining two series together is doubtful (Fig. 9b).

Interestingly, both the trends of annual TCs in Japan and affecting HK during the past 110 years plus showed a similar decrease (−0.08 and −0.11 TC/10 years, respectively). They support the previous findings that the TC frequency in Western Pacific has not increased under the background of global warming since the late nineteenth century (Chan and Liu 2004; Gao et al. 2007; Nagata and Mikami 2017), and the number of TCs affecting southern China coastal zone and the TC-caused precipitation in China mainland has actually decreased over the last 5–6 decades (Ren et al. 2007), though the more intense typhoons and the more extreme precipitation caused by them in China's mainland may have increased during the same time period (Yu et al. 2009; Kossin 2018; Lai et al. 2020).

Table 4 The variation of the number of annual TCs affecting Fujian and HK during 1884–2017

Influence area	1884–1902	1903–1931	1932–1955	1956–1971	1972–2003	2004–2017	Source
Fujian	4.1	5.3	4.3	6.2	4.7	–	Gao et al. 2007
HK	4.6 (1885–1902)	5.0	4.2 (missing 1940–1946)	4.6	3.9	4.1	OIM

Table 5 The trends of the number of annual TC landfalls or TCs having influences over East Asia (in TCs per 10 years) in Figs. 8 and 9

Trend	Period	Landing/influence area	Source
0.42	1885–1939	China	Gao and Zeng 1957
0.00		HK	OIM
−0.34	1949–2016	China	CMA-BST
−0.09		HK	OIM
0.07	1885–2016	China	Merged CMA-BST and Gao and Zeng 1957 together
−0.08		HK	OIM
−0.08	1900–2014	Japan	Kumazawa et al. 2016
−0.11		HK	OIM

The significant trends at the 0.05 confident level are italicized

5 Conclusions

The long series of TCs over mainland China was inhomogeneous since the late nineteenth century due to the lack of consistently observational records during the different stages. In this study, we developed an objective identification method for TC reconstruction by using observed SAP data, and HK station was taken as an example. Main results of this study are as follows.

1. For HK station, the average distance (i.e., CDD) of detectable landing TC is 362 km. This means that, on average, the TCs within this distance were supposed to have significant impacts on the SAP change at HK station and vice versa. Definitely, this is only the general distance obtained from statistics, and a few strong TCs, even though they are not within this range, still have significant impacts on the SAP change of HK. Meanwhile, a few weak TCs within this distance do not have much impact on HK in terms of SAP due to their weak intensity.
2. The thresholds of daily mean SLP and the absolute value of 24-h SLP difference for HK station to indicate a TC influence were determined as 1004.2 hPa and 3.4 hPa, respectively. These two SLP thresholds were applied to the SLP records during the period of 1885–2017 at HK station, and a homogenous 133-year series of TCs that have impacts on HK was reconstructed and affirmed applicable for use in studies of climate change.
3. The reconstructed series of TCs from 1885 to 2017 indicated an apparent decreasing trend accompanied by obvious inter-annual to multi-decadal variability. The number of TCs affecting HK during the early 1910s to the 1930s was more than the climatological mean and was apparently less than the climatological mean from the early 1990s to the early 2000s. Significantly, TCs affecting HK dramatically decreased after 1993, and the number is higher than the climatological mean only in 4 of the 24 years. This result is consistent with the previous findings that the TC frequency in western North Pacific has not increased under the background of global warming since the late nineteenth century.

Following this study, we plan to apply this method to the available SAP records at more stations in East Asia or China in order to build a long regional TC series especially covering the pre-1950 stage. Definitely, if more climatic variables during the early years such as wind speed or precipitation data would be rescued, it will be helpful to reduce the misjudgment rate of the objective identification of TCs in the region.

Acknowledgements NMIC and STI of CMA, and ISPD provided the data used in the study. We are also grateful to the three anonymous reviewers for their valuable comments and guidance that greatly improved this manuscript.

Funding This work was sponsored by the National Key Research and Development Program of China (grant numbers 2018YFA0605603 and 2016YFA0600301).

References

Barcikowska M, Feser F, Zhang W, Mei W (2017) Changes in intense tropical cyclone activity for the western North Pacific during the last decades derived from a regional climate model simulation. Clim Dyn 49:2931–2949. https://doi.org/10.1007/s00382-016-3420-0

Briffa KR, Jones PD (1993) Global surface air temperature variations during the twentieth century: part 2, implications for large-scale high-frequency palaeoclimatic studies. Holocene 3:77–88. https://doi.org/10.1177/095968369300300109

Chan JCL, Liu KS (2004) Global warming and western North Pacific typhoon activity from an observational perspective. J Clim 17:4590–4602. https://doi.org/10.1175/3240.1

Chan JCL, Shi E (2000) Frequency of typhoon landfall over Guangdong Province of China during the period of 1470–1931. Int J Climatol 20:183–190

Chin PC (1972) Tropical cyclone climatology for the China seas and Western Pacific from 1884 to 1970. Royal Observatory, Hong Kong

Fogarty EA, Elsner JB, Jagger TH, Liu KB, Louie KS (2006) Variations in typhoon landfalls over China. Adv Atmos Sci 23:665–677. https://doi.org/10.1007/s00376-006-0665-2

Gao YX, Zeng YE (1957) Typhoon tracks map and some statistics (in Chinese). Science Press, Beijing

Gao JY, Jiang ZH, You LJ, Zhang RY (2007) Variations in activities of Fujian-affecting tropical cyclones during 1884-2003 (in Chinese with English abstract). J Appl Meteor Sci 18(2):211–218. https://doi.org/10.11898/1001-7313.20070211

Grossman M, Zaiki M (2009) Reconstructing typhoons in Japan in the 1880s from documentary records. Weather 64:315–322. https://doi.org/10.1002/wea.401

Hofstra N, Haylock M, New M, Jones P, Frei C (2008) Comparison of six methods for the interpolation of daily, European climate data. J Geophys Res 113:D21110. https://doi.org/10.1029/2008JD010100

Hung CW (2013) A 300-year typhoon record in Taiwan and the relationship with solar activity. Terr Atmos Ocean Sci 24:737–743. https://doi.org/10.3319/TAO.2013.02.18.01(A)

Jones PD, Osborn TJ, Briffa KR (1997) Estimating sampling errors in large-scale temperature averages. J Clim 10:2548–2568

Kobayashi Y, Pan W (2014) Reconstruction of 2 significant typhoon paths in the 17th century Japan (in Chinese with English abstract). J Earth Environ 5(6):363–369

Kossin JP (2018) A global slowdown of tropical-cyclone translation speed. Nature 558:104–107. https://doi.org/10.1038/s41586-018-0158-3

Kumazawa R, Fudeyasu H, Kubota H (2016) Tropical cyclone landfall in Japan during 1900-2014 (in Japanese with English abstract). TENKI 63:855–861 https://www.metsoc.jp/tenki/pdf/2016/2016_11_0003.pdf

Ladlow C, Woodruff JD, Cook TL, Baranes H, Kanamaru K (2019) A fluvially derived flood deposit dating to the kamikaze typhoons near Nagasaki, Japan. Nat Hazards 99:827–841. https://doi.org/10.1007/s11069-019-03777-z

Lai YC, Li JF, Gu XH, Chen YQD, Kong DD, Gan TY, Liu MF, Li QQ, Wu GF (2020) Greater flood risks in response to slowdown of tropical cyclones over the coast of China. PNAS 117:201918987. https://doi.org/10.1073/pnas.1918987117

Liu KS, Chan JCL (2008) Interdecadal variability of western North Pacific tropical cyclone tracks. J Clim 21:4464–4476. https://doi.org/10.1175/2008JCLI2207.1

Liu KB, Shen CM, Louie KS (2001) A 1,000-year history of typhoon landfalls in Guangdong, southern China, reconstructed from Chinese historical documentary records. Ann Assoc Am Geogr 91(3):453–464

Louie KS, Liu KB (2003) Earliest historical records of typhoons in China. J Hist Geogr 29:299–316. https://doi.org/10.1006/jhge.2002.0453
Nagata R, Mikami T (2017) Reconstruction of typhoon tracks around Japan using daily precipitation data, 1901-2000 (in Japanese). Annual Meeting of the Association of Japanese Geographers, Spring 2017. https://doi.org/10.14866/ajg.2017s.0_100006
Pan W, Wang MS, Man ZM, Cui JX (2012) Reconstruction of the affecting East China typhoon frequency, 1644~1911 AD (in Chinese with English abstract). Resources and Environment in the Yangtze Basin 21(2): 237–241
Ren F, Wang Y, Wang X (2007) Estimating tropical cyclone precipitation from station observations. Adv Atmos Sci 24(4):700–711. https://doi.org/10.1007/s00376-007-0700-y
Ren ZH, Yu Y, Zou FL, Xu Y (2012) Quality detection of surface historical basic meteorological data (in Chinese with English abstract). J Appl Meteor Sci 23(6):739–747
Wang XL, Chen H, Wu Y, Pu Q (2010) New techniques for detection and adjustment of shifts in daily precipitation data series. J Appl Meteor Climatol 49(12):2416–2436. https://doi.org/10.1175/2010jamc2376.1
Williamson F, Allan R, Ren G, Lee TC, Lui WH, Kubota H, Matsumoto J, Luterbacher J, Wilkinson C, Wood K (2018) Collating historic weather observations for the East Asian region: challenges, solutions and reanalyses. Adv Atmos Sci 35:899–904. https://doi.org/10.1007/s00376-017-7259-z
Willmott CJ, Clinton MR, Philpot WD (1985) Small-scale climate maps: a sensitivity analysis of some common assumptions associated with grid-point interpolation and contouring. Am Cartographer 12:5–16. https://doi.org/10.1559/152304085783914686
Xue XY, Ren GY, Sun XB (2019) Climatological characteristics of meso-scale and micro-scale strong convective weather events in China (in Chinese with English abstract). Climatic Environ Res 24(2):59–73. https://doi.org/10.3878/j.issn.1006-9585.2018.17148
Ying M, Zhang W, Yu H, Lu X, Feng J, Fan Y, Zhu Y, Chen D (2014) An overview of the China Meteorological Administration tropical cyclone database. J Atmos Ocean Technol 31:287–301. https://doi.org/10.1175/JTECH-D-12-00119.1
Yu Z, Yu H, Chen P, Qian C, Yue C (2009) Verification of tropical cyclone–related satellite precipitation estimates in mainland China. J Appl Meteor Climatol 48:2227–2241. https://doi.org/10.1175/2009JAMC2143.1
Zhang XP, Ye Y, Fang XQ (2012) Reconstruction of typhoons in the Yangtze River Delta during 1644–1949AD based on historical chorographies. J Geogr Sci 22(5):810–824. https://doi.org/10.1007/s11442-012-0965-7
Zhang Y, Hidalgo J, Parker D (2017a) Impact of variability and anisotropy in the correlation decay distance for precipitation spatial interpolation in China. Clim Res 74:81–93. https://doi.org/10.3354/cr01486
Zhang QH, Ni X, Zhang FQ (2017b) Decreasing trend in severe weather occurrence over China during the past 50 years. Sci Rep 7:42310. https://doi.org/10.1038/srep42310
Zhu Q, Lin J, Shaowen S, Dongsheng T (2000) Principles and methods of synoptic meteorology (in Chinese). China Meteorological Press, Beijing